[12] J. Christian and G. Goubau, "Experimental studies on a beam waveguide for millimeter waves," IRE TRANS. ON ANTENNAS AND PROPAGATION, vol. AP-9, pp. 256–263; May, 1961.
[13] J. Christian and G. Goubau, "Some measurements on an iris beam waveguide," PROC. IRE (*Correspondence*), vol. 49, pp. 1679–1680; November, 1961.
[14] J. Beyer, "Study of the Beam Waveguide," Ph.D. thesis, University of Wisconsin, Madison, 1961; University Microfilms, Inc., Ann Arbor, Mich. A portion of this work has been published: J. Beyer and E. Scheibe, "Loss measurements of the beam waveguide," IEEE TRANS. on MICROWAVE THEORY AND TECHNIQUES, vol. MTT-11, pp. 18–22; January, 1963.
[15] J. Beyer and E. Scheibe, "Higher modes in guided electromagnetic wave beams," IRE TRANS. ON ANTENNAS AND PROPAGATION (*Correspondence*), vol. AP-10, pp. 349–350; May, 1962.
[16] Y. Beers, R. Zimmerer, G. Strine, and M. V. Anderson, "Millimeter wavelength resonant structures," IEEE TRANS. ON MICROWAVE THEORY AND TECHNIQUES, vol. MIT-11, pp. 142–149; March, 1963. See also, W. Culshaw, "Resonator for millimeter and submillimeter wavelengths," IEEE TRANS. ON MICROWAVE THEORY AND TECHNIQUES, vol. MTT-9, pp. 135–144; March, 1961.
[17] The use of ellipsoidal microwave cavities has not been extensive. This is in part due to the difficulty of theoretical anlaysis. Two such theoretical investigations are recorded in the literature and pertain to this discussion. The word confocal is used both in its geometrical sense as confocal ellipses and optical sense of lenses having a common focal point. J. C. Simons, "Electromagnetic Resonant Behavior of a Confocal Spheroidal Cavity System in the Microwave Region," Ph.D. thesis, M.I.T., Cambridge; 1950. H. Geppert and H. Schmid, "Confocal Ellipsoidal Shells as Electromagnetic Cavity Resonators," Wartime Rept. of the Mathematical Institute of the University of Berlin, Germany; available from ASTIA as Document ATI 32573, May, 1944.
[18] C. Flammer, "Spheroidal Wave Functions," Stanford University Press, Palo Alto, Calif., Ch. 8.2; 1957.
[19] See for example the discussion of the Scalar wave equation in elliptic cylinder coordinates for $b \gg \lambda$ in P. Morse and H. Feshbach, "Methods of Theoretical Physics," McGraw-Hill Book Co , Inc., New York, N. Y., pp. 1416–1420; 1953.
[20] E. Pinney, "Electromagnetic fields in a paraboloidal reflector," *J. Math. and Phys.*, vol. 26, pp. 42–55; 1947.
[21] J. R. Pierce, "Theory and Design of Electron Beams," D. Van Nostrand and Co., New York, N. Y.; 1954.
[22] ——, "Modes in sequences of lenses," *Nat'l. Acad. of Sci.*, vol. 47, pp. 1808–1813; November, 1961.
[23] The conventional use of r, R and z, Z and x, X in the following discussion to represent impedance and reactance should not be confused with the earlier use of the same symbols for coordinates.
[24] This particular application is discussed in C. G. Montgomery, R. H. Dicke, and E. M. Purcell, "Principles of Microwave Circuits," McGraw-Hill Book Company, Inc., New York, N. Y. sec. 7.10; 1948.
[25] E. Rosenblum, "Atmospheric absorption of 10-400 Gcs radiation," *Microwave J.*, vol. 4, pp. 91–96; March, 1961.
[26] R. Zimmerer, "New wavemeter for millimeter wavelengths," *Rev. Sci. Instr.*, vol. 33, pp. 858–859; August, 1962.

Microwave Type Bolometer for Submillimeter Wave Measurements*

J. F. BYRNE†, FELLOW, IEEE, AND C. F. COOK‡

***Summary*—An approach to the problem of submillimeter wave measurement through the extension of microwave techniques has led to the development of a submillimeter bolometer with the sensitivity requisite to calibration with a thermal source. The sensor employs conventional components, horn, waveguide and coaxial line, with a novel coax-to-guide transition consisting of part of the bolometer element, the rest of which serves as a center conductor of the coaxial lines. The entire set of submillimeter components is contained in a ¼-inch block of metal. Fundamental problems of detection in this band are discussed with application to the sensor. Calibration techniques and data taken with the instrument are reported.**

INTRODUCTION

THE SENSOR described in this paper is the outcome of an effort to provide a method of measurement of radiation in the wavelength region around and below one millimeter. In approaching the problem of submillimeter wave measurement it was decided that the equipment design might well be benefited through the extension of microwave technologies into this portion of the spectrum rather than the alternate approach which would be to attack the problem from the infrared point of view.

A prime advantage of the microwave view was the likelihood that the number of unknown quantities could be minimized through the almost exclusive use of metallic elements in the system. The bolometer design finally adopted essentially consists of a horn antenna feeding a submillimeter waveguide which is terminated in a novel waveguide to coax transition section. The coaxial section has a center conductor of Wollaston wire of extremely small size and high loss per unit length. The termination of the coaxial section is of little importance because of the high loss along the coax. The waveguide is thus terminated in a transition to coax with a "lossy" line as the load.

SENSOR CONFIGURATION

Fig. 1 shows the sensor configuration. The bolometer wire serves both as the center conductors of the two lossy coaxial lines and the probe which couples the waveguide and the coax system. The probe crosses the wave-

* Received January 21, 1963. This paper was presented at the IEEE Millimeter and Submillimeter Conference, Orlando, Fla. January 7–10, 1963.
† Motorola Inc., Technical Products Divisions, Phoenix, Ariz.
‡ Motorola Inc., Systems Research Laboratory, Riverside, Calif.

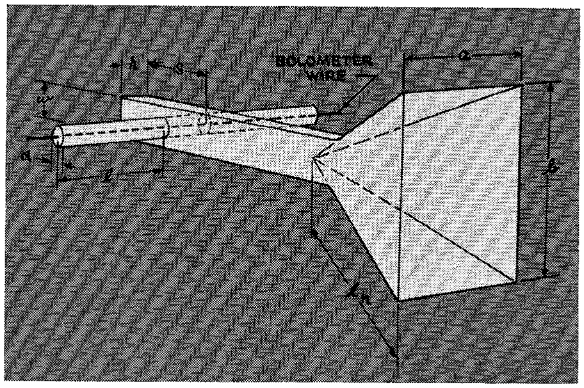

Fig. 1—Diagram of sensor.

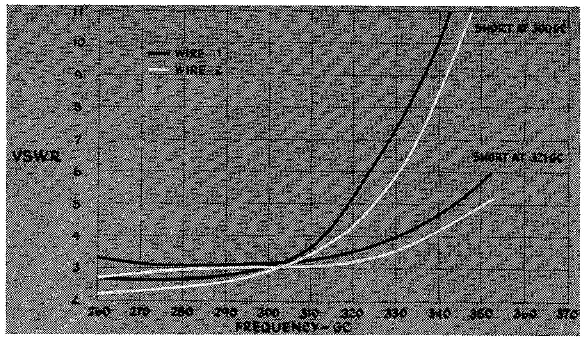

Fig. 2—VSWR computed from X-band model of sensor.

guide at a distance approximately $\frac{1}{4}$-guide wavelength from the shorted end of the guide.

In optimum design, the characteristic impedance of each coaxial line should be one half the characteristic impedance of the waveguide. In the case of a rectangular waveguide with a conventional height-to-width ratio of one half, the required ratio of coaxial outer-to-inner conductor diameter becomes approximately 30. The platinum wire bolometer element is 25 one millionths of an inch in diameter, or 6300 A units. At the 30 to 1 ratio the outer diameter d of the line becomes 0.75 mil which was considered too small for practical fabrication with existing facilities. A two-to-one impedance mismatch, which would introduce a one-half decibel error in measurement, would occur if the ratio were raised to 300. The waveguide dimensions for the unit with a 1-mm band center are 0.016-inch high and 0.032-inch wide. The guide wavelength at band center is 0.065 inch. The bolometers produced to date have been dimensioned for simple construction and a two-to-one mismatch has been considered quite tolerable. Increase of guide height could, of course, improve the match, but better waveguide mode control is achieved with the guide proportions currently employed.

To check the feasibility of the configuration and to find the optimum position (s) for the probe, an X-band model was constructed. The VSWR was obtained for the model using several values of s. Difficulty was encountered in obtaining wire which had both the correct value of resistance per unit length and the correct diameter; it was possible to find wire with the correct diameter and wire with the correct resistance per unit length, so the test was made with each. A movable shorting bar was included to change s.

Fig. 2 shows the VSWR measured on these models as a function of frequency. We see that the position of the probe has a much greater effect than the difference between wires, and that there is a reasonably wide region with an acceptable VSWR if we select a position of the probe to favor the high-frequency end of the band.

The horn need not be optimum with respect to length, since size is not a problem; a narrow horn with high efficiency and a beamwidth narrow enough to illuminate a thin lens with a minimum of reflection and dielectric losses is desirable.

Fig. 3 shows the structural arrangement required to assemble the sensor. The unit is cut in half down the axis and parallel to the electric plane of the guide, which insures that there is no conduction current flow across the metallic junction. Each half is a single block of metal. The bolometer wire is mounted on one half and adjusted properly before the two are joined.

Coining the horn and waveguide into the block leaves fine surfaces, avoids conduction joints and assures accurate duplication of the sensor. Because little is known about the losses caused by insulating surface coatings at these frequencies, the sensor is gold-plated and left as clean as possible. To prevent the bolometer wire from becoming shorted to the walls of the coaxial line and to maintain the concentricity of the line, the wire is stretched through the cavity with springs which keep a constant tension of about one dyne in the wire, which is about 10 per cent of the ultimate strength of the wire.

To obtain the sensitivity required for the use of heat sources for signal generators, it is necessary to prevent energy loss by conduction to any gas in the cavity. Therefore no materials are used which are not stable in a vacuum or cannot withstand baking at a high enough temperature to outgas them. Quartz and Vycor glass were found to be satisfactory window material for the vacuum capsule.

Two models of the sensor have been produced with overlapping frequency ranges, one with band center at 300 Gc, the other with band center at 225 Gc. They are identical except for the horn and waveguide dimensions. The important dimensions and electrical properties at center frequency of the 300-Gc model are

Bolometer wire

length ($2l+h$)	0.25 inch
diameter	0.025 inch
dc resistance	9.0 ohms/mil
resistance at 300 Gc	8.24 ohms/mil
temperature coefficient of resistance	0.003/°C

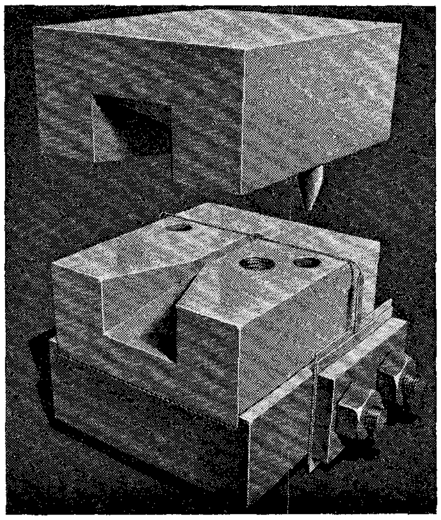

Fig. 3—Submillimeter sensor.

Coaxial Line	
length (l)	0.117 inch
outer conductor (d)	8 mil
inner conductor	0.025 mil
impedance	345 ohms
attenuation	0.10 db/mil
total attenuation	12 db
Horn	
H-plane opening (b)	130 mil
E-plane opening (a)	103 mil
H-plane beamwidth	23° (for 300 Gc)
E-plane beamwidth	22° (for 300 Gc)
effective area	4.2 mm²
Waveguide	
height (h)	16 mil
width (w)	32 mil
distance from shorted end of waveguide to probe (s)	12 mil
characteristic impedance	375 ohms
$\frac{\lambda_g}{\lambda}$	1.63
cutoff frequency	184 Gc.

Theory of Operation

In the early experimental work, a conventional bridge circuit employing 1000-cps excitation was employed and was only moderately satisfactory. The "no signal" balance was highly temperature sensitive and annoyingly unstable. Because of these problems, a low-frequency ac system was chosen, in which the signal to be measured was modulated at a low frequency which was compatible with the bolometer thermal time constant. The circuit is arranged so that a constant, highly stable, "quiet," direct current is employed for bolometer bias. Under this condition, the bolometer voltage is a direct function of bolometer resistance, or bolometer temperature. When the amplitude of the radiation incident upon the bolometer is varied at the prescribed frequency, its temperature and hence terminal voltage will likewise vary. This voltage is then detected by any one of a variety of means. The appropriate frequency for signal amplitude modulation is determined on the high side by the thermal time constant of the bolometer, and, because of the $1/f$ noise of vacuum tubes or other amplifiers, operation near the upper-frequency limit is preferred. In the case of the 25-μinch Wollaston wire, this frequency is in the 2- to 3-cps range.

The signal input to the bolometer is conveniently modulated by a rotating Faraday screen placed in the signal path. The signal power is then modulated in accordance with the following equation:

$$P = \frac{P_0(1 + \sin\theta)}{2} = \frac{P_0}{2} + \frac{P_0 \sin\theta}{2} \tag{1}$$

where

P_0 = steady unmodulated signal power level

θ = angle between the signal electric vector and the screen wire.

With the screen rotating, this becomes

$$P = \frac{P_0}{2} + \frac{P_0}{2} \sin\omega t \tag{2}$$

where

$\frac{\omega}{2\pi}$ = modulating frequency

$\frac{\omega}{4\pi}$ = rotational frequency of the screen system.

The voltage output of the bolometer at low signal levels is proportional to the signal power input, and its response is limited by the thermal time constant.

Bolometer output voltage

$$= \frac{K_b P_0}{2} + \frac{K_b P_0 \sin\omega t}{2\sqrt{1 + (\omega\tau)^2}} \tag{3}$$

$$= \frac{K_b P_0}{2}\left[1 + \frac{\sin\omega t}{\sqrt{1 + (\omega\tau)^2}}\right] \tag{4}$$

where

K_b = bolometer calibration constant

τ = bolometer thermal time constant.

The rotating Faraday screen also has the desirable property of modulating all frequencies below that at which the wire spacing is approximately $\frac{1}{3}$ of a wavelength, and producing diminishing amounts of modulation for all frequencies above that value. Hence, infrared radiation is substantially unmodulated and is not effective in producing a bolometer ac output. The low-frequency response of the bolometer is, of course, determined by waveguide dimensions.

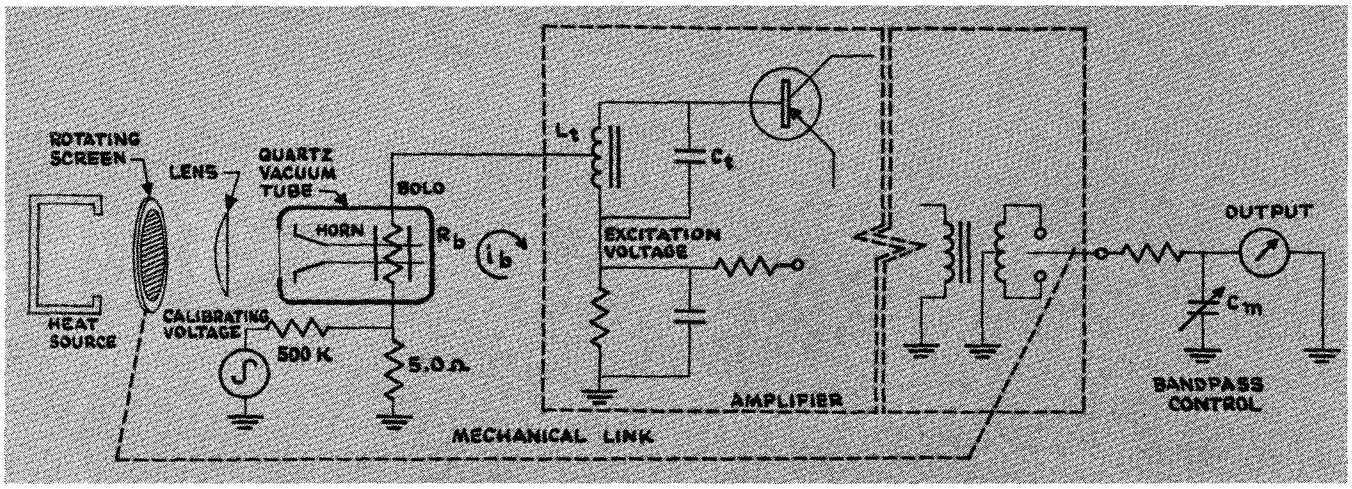

Fig. 4—Measurement system. Statement of power equilibrium in bolometer wire.

$$\pi R^2 K \frac{d^2 \Delta T}{dx^2} + 2\pi \sigma \epsilon_1 \left[(T_0 + \Delta T)^4 - T_0^4\right] - \frac{i^2 \rho (1 + \propto \Delta T)}{\pi R^2} = 0\cdot$$

A system diagram is shown in Fig. 4. The energy enters the system through a collecting lens or mirror, passes through the modulating screen, enters the vacuum capsule through the quartz window heating the bolometer wire and causing a change of resistance ΔR_b. The product of the excitation current i_0 with ΔR_b is a sinusoidal voltage with a value v proportional to the signal power in the bolometer. The inductance L_t of the input transformer is resonated with capacitor C_t to maximize v and narrow the bandwidth of the input noise.

A synchronous filter, operated mechanically from the rotating screen, has been found to be effective, the pass band being regulated by the size of C_m.

It would be desirable to compute the optimum value of i_0 and the sensitivity of the instrument from the circuit parameters, but the calculation of v presents some difficulty. The bolometer differs from a conventional bolometer in that signal power is not dissipated uniformly along the wire but exponentially about the center, such that half the power is dissipated in the center quarter of the wire. In addition, the precise calculation of the temperature of the wire, as a function of length along the wire and input power, is quite complicated as shown below. The equation for the steady-state balance of power entering and leaving the element dx of the bolometer wire of length $2l_b$ is[1]

$$\pi r^2 K \frac{d^2 \Delta T}{dx^2} + 2\pi r \epsilon_1 \sigma \left[(T_0 + \Delta T)^4 - T_0^4\right] - \frac{(\alpha \Delta T + 1) i^2(x) \rho}{\pi r^2} = 0, \quad (5)$$

where

x = distance from center of wire
K = coefficient of conductivity
r = radius of wire
ϵ_1 = effective emittance of wire
α = temperature coefficient of resistance $(1/\rho)(d\rho/dT)$
ρ = resistivity of wire
$i(x)$ = current in wire
$T = T_0 + \Delta T$ = temperature of wire (Kelvin)
T_0 = ambient temperature.

We have good values for all the coefficients except ϵ_1, the effective emittance of the bolometer wire in its environment. The emittance is a function of the shape of the wire and its surface texture. Its environment includes its position almost on the axis of a nearly cylindrical polished cavity where the reflected power density is a maximum. The wire diameter is much smaller than the wavelength of the peak of the black body power distribution for its temperature, so that the macroscopic properties of emissivity for the material probably do not hold. Having no way of estimating the proper value of ϵ_1, we find the general nature of the distribution of power in the wire using the maximum value one. For the excitation power alone, where i_0 is independent of x, solutions are easy to obtain with the analog computer. For arbitrary values of $i_0^2\rho$ and T_0 we find families of solutions for ΔT and $\int \Delta T dt$ as functions of x, as shown in Fig. 5. The value of x when T is zero is l_b. We now plot ΔT_0 and $\int \Delta T dt / l_b = \Delta T_a$ as functions of l_b given in Fig. 6, and read from these ΔT_0 and ΔT_a as functions of $i_0^2\rho$. These appear in Fig. 7. Now

$$\Delta T_a = R_b \frac{dT}{dR} = \frac{1}{6.3} R_b$$

[1] R. A. Smith, S. E. Jones and R. P. Chasmar, "The Detection and Measurement of Infra-Red Radiation," Oxford University Press, New York, N. Y., p. 103; 1957.

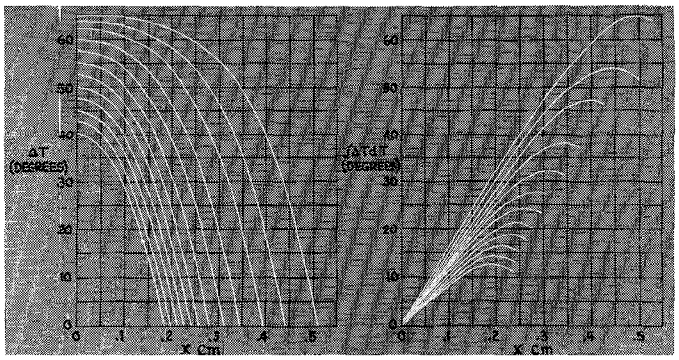

Fig. 5—Computations of ΔT and $\int \Delta T dx$.

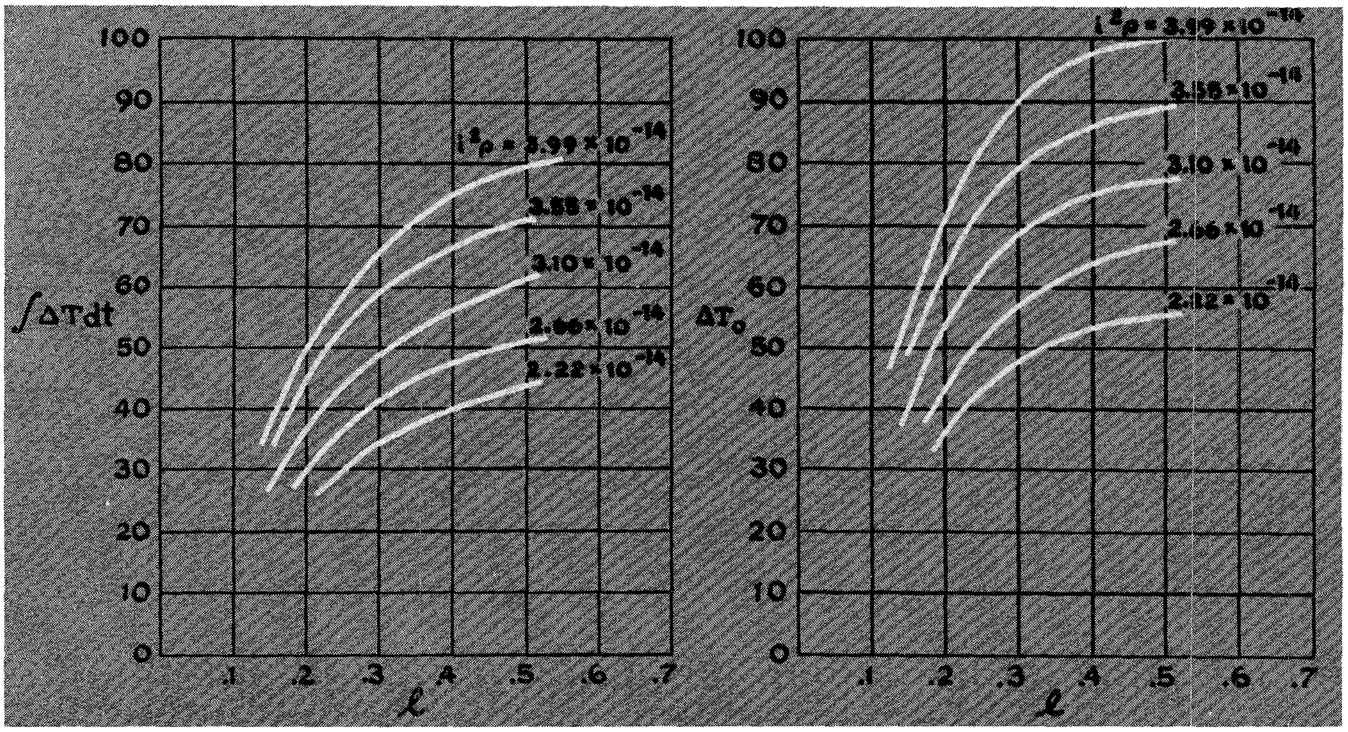

Fig. 6—ΔT_0 and $\int \Delta T dt$ as function of l.

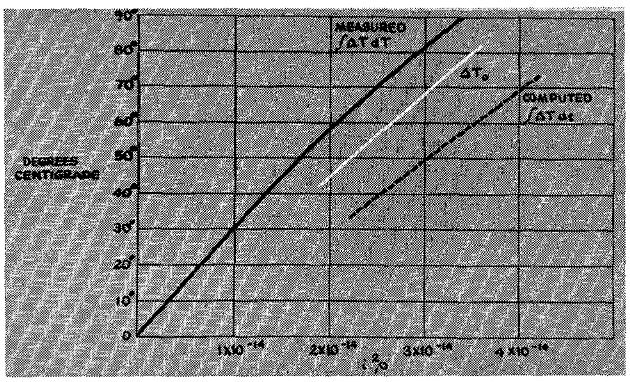

Fig. 7—Computed and measured bolometer wire temperature.

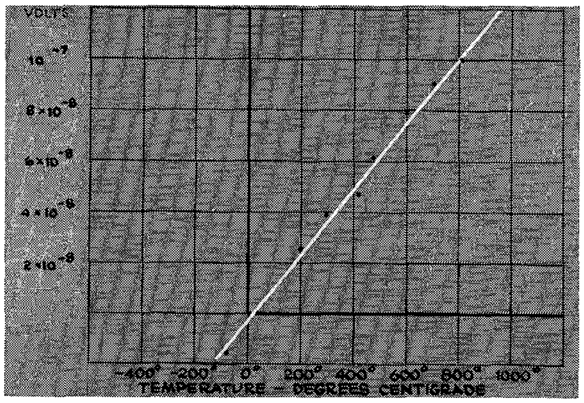

Fig. 8—Calibration of sensor No. 3.

can be determined experimentally and is shown with ΔT_a in Fig. 7. We notice that the experimental value is considerably higher than the computed value, which is the correct direction to be the result of an ϵ_1 less than one, but no corroborating experiments have been made. It appears that for the present we must be satisfied with an experimental calibration.

Experimental Calibration of the Sensor

A small metallurgical furnace with temperature range to 1000°C and thermostatic control provides a good calibration source. In the temperature range of this experiment, it can be shown that if the aperture of the black body subtends the entire beam pattern of the receiver, the maximum available power at the bolometer is $kT\Delta f$ where k is the Boltzmann constant, T is the absolute temperature and Δf is the bandwidth of the transmission path. Since the ac amplifier eliminates all but the modulated component of the signal, T becomes the difference between the temperature of the region from which energy is reflected into the sensor by the modulating screen and the temperature of the body transmitting energy through the screen.

In calibrating, we first showed that the sensor output was independent of the distance to the black body over the proper range to prove that the beamwidth condition had been met; then the data given in Fig. 8 were recorded by matching the bolometer readings with a calibrating voltage introduced in a manner similar to that shown in Fig. 4.

On the calibration curve of Fig. 8, the point at $-70°$ was obtained by substituting a box of dry ice for the furnace. The slope of this curve is the temperature sensitivity which can be converted to power sensitivity provided the bandwidth is known. We estimate the bandwidth for this sensor to be about one octave or 2×10^{11} cps, which we have verified by an independent technique that we expect to report later. Using this number we arrive at a calibration constant for the system of 196 volts peak-to-peak per watt of input power. This number includes the effects of the losses due to reflection from the lens and window, modulator polarization, mismatch at the probe and thermal time constant of the wire. With the bandwidth of the amplifier adjusted to $\frac{1}{20}$ cps we find the corresponding noise amplitude to be about 6×10^{-9} volts which indicates that we can recognize an input power of about 3×10^{-11} watts with the equipment used, a figure which is verified by the deviation of calibration points on the curve of Fig. 8.

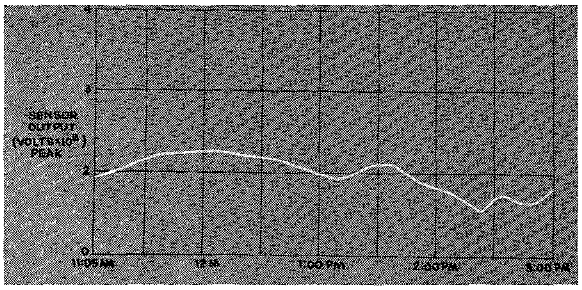

Fig. 9—Millimeter wave signal received from sun (August 10, 1962).

The sensitivity of the bolometer element should be estimated from consideration of the noise figures of the amplifier and the attenuation of the path of the signal, which are between 12 and 13 db for the amplifier and between 5 and 7 db for the optical path and coupling. These losses can be decreased if the optics are optimized for single frequency use with grooved surfaces and if a better amplifier is supplied. A parametric amplifier with a 0.3-db noise figure is reported.[2] If current noise does not become important, it appears probable that a sensitivity of 5×10^{-12} watts can be achieved.

Measurements

Having a sensor and a source of radiation, it becomes possible to measure transmission characteristics of dielectric materials and to find sources of radiation. The output of a high pressure quartz mercury lamp is a better source of radiation than the furnace, so that it has been used for most of the measurements of dielectrics. We have determined the optical characteristics of the materials which are in use as lenses and windows. For example, some materials which have been found to be transparent are teflon, paraffin, quartz, polystyrene and solid carbon dioxide. Materials which are relatively opaque are lantern slide glass, pyrex, sapphire, water, common ice and epoxy.

Fig. 9 gives the intensity of radiation from the sun at an altitude of 800 feet through part of one day, recorded by a clock-driven telescope with a 6-inch teflon lens.

Our work indicates that the microwave techniques can be extended into the submillimeter region and that this sensor may become a valuable tool for the detection and measurement of submillimeter wave power.

[2] J. R. Biard, "Low-frequency reactance amplifier," IEEE Trans. on Microwave Theory and Techniques, vol. MTT-11, pp. 298–303; February, 1963.